Chinese Chemical Letters 33 (2022) 328–333

Contents lists available at ScienceDirect

Chinese Chemical Letters

journal homepage: www.elsevier.com/locate/cclet

An *in situ* nanoparticle recombinant strategy for the enhancement of photothermal therapy

Xinxin Liu[a,b,c,d,e], Cuixia Zheng[b,c,d], Yueyue Kong[b,c,d], Hao Wang[b,c,d], Lei Wang[a,b,c,d,e,*]

[a] *Luoyang Central Hospital Affiliated to Zhengzhou University, Luoyang 471009, China*
[b] *School of Pharmaceutical Sciences, Zhengzhou University, Zhengzhou 450001, China*
[c] *Key Laboratory of Advanced Drug Preparation Technologies, Ministry of Education, School of Pharmaceutical Sciences, Zhengzhou University, Zhengzhou 450001, China*
[d] *Henan Key Laboratory of Targeting Therapy and Diagnosis for Critical Diseases, Zhengzhou University, Zhengzhou 450001, China*
[e] *Tumor Immunity and Biomaterials Advanced Medical Center, Zhengzhou University, Luoyang 471009, China*

ARTICLE INFO

Article history:
Received 17 May 2021
Revised 2 July 2021
Accepted 7 July 2021
Available online 14 July 2021

Keywords:
Photothermal therapy
Tumor-associated antigens
Recombinant nanoparticle
T cells activation
Individual immunotherapy

ABSTRACT

Photothermal therapy (PTT)-induced immune response has attracted much attention, however, which cannot work at full capacity. In this study, the simvastatin (SV) adjuvant is loaded into gold nanocages (AuNCs) to develop a simple drug delivery system, which can efficiently utilize the tumor-associated antigens (TAAs) for improving immune responses. AuNCs/SV-mediated PTT treatment enhances tumor cells damage and promotes the release of TAAs which are immediately captured by AuNCs/SV to form AuNCs/SV/TAAs recombinant nanoparticle. Impressively, AuNCs/SV/TAAs can accumulate in lymph nodes effectively due to the suitable size of ~55 nm and hyperthermia-induced vasodilative effect. And the co-delivery of antigen and adjuvant is beneficial to stimulating the maturation of dendritic cells for further activating T cells. In a word, the recombinant strategy could make full use of TAAs to produce an individual powerful immunotherapy.

Currently, cancer is still one of the diseases with high morbidity and mortality in the world [1–4]. Recently, as an important cancer treatment method, photothermal therapy (PTT) based on nanomaterials has attracted much attention because of its minimally invasive, high efficiency and few adverse reactions [5–9]. PTT could induce dying tumor cells to release tumor-associated antigens (TAAs) and damage-associated molecular model (DAMPs) to stimulate the host immune system [10–12]. However, the immune response induced by hyperthermia is relatively weak and short-lived [13]. At present, how to make better use of TAAs produced in the process of PTT is very important to amplify the immune effect induced by PTT.

Researches have showed that nanoparticles (NPs) could enhance immune response due to the effective delivery of antigen and/or adjuvant [14–17]. For example, large-pore mesoporous organosilica nanospheres could deliver antigens to dendritic cells (DCs) and then activate DCs effectively [18]. Polymer/lipid NPs could also mediate the retention of vaccine cargo in DCs, enhancing DCs activation and the body's immune response [19]. Unfortunately, traditional nanovaccines are always using the pre-extracted antigens which are complicated and costly, limiting their applications [20–22]. Using TAAs produced by PTT to construct recombinant vaccine-like NPs in tumor site can not only solve the above problem, but also improve the therapeutic efficiency of PTT.

As one of the PTT intensifiers, gold nanocages (AuNCs) with hollow mesoporous structure and unique surface property are suitable for small molecule drugs loading and protein capture, which are beneficial for the protection of adjuvant and TAAs [23–27]. Besides, AuNCs can migrate to lymph nodes (LNs) easily due to the size of 20~100 nm and PTT-induced blood vessels dilatation, which are beneficial to activating systemic immune response [28,29].

Herein, AuNCs/SV NPs were constructed by placing simvastatin (SV) adjuvant in the cavity of AuNCs. SV is a mevalonate pathway inhibition-based immunological adjuvant, known to increase antigen presentation *via* prolonged antigen preservation during endocytosis [30]. With the irradiation of near-infrared (NIR) laser, tumor could be killed by AuNCs/SV directly and released TAAs that would be captured by AuNCs/SV to construct an *in situ* NPs (AuNCs/SV/TAAs). AuNCs/SV/TAAs of ~55 nm could be advantageous to migrate to the LNs, especially with the help of PTT-induced vasodilation, and ingested by DCs to promote the differentiation of $CD4^+$ T cells and $CD8^+$ T cells (Fig. 1). In general, this

* Corresponding author.
E-mail address: wanglei1@zzu.edu.cn (L. Wang).

https://doi.org/10.1016/j.cclet.2021.07.025
1001-8417/

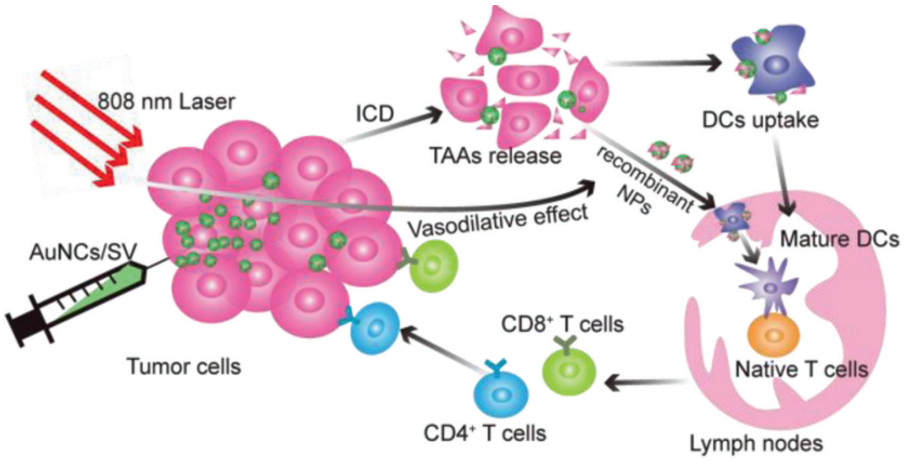

Fig. 1. Schematic overview of the construction of *in situ* recombinant nanoparticle with lymph node-targeting ability for enhancing PTT-immunotherapy.

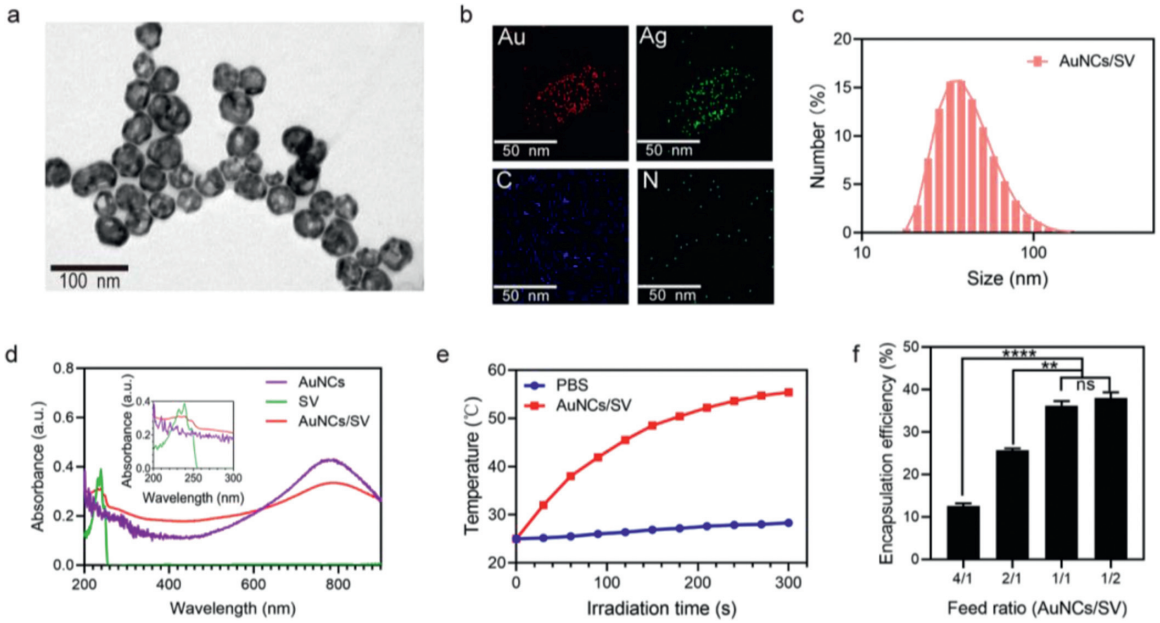

Fig. 2. (a) TEM image and (b) Elemental mapping of AuNCs. (c) Size of AuNCs. (d) UV-vis spectra of SV, AuNCs and AuNCs/SV. The insert image was a magnified figure of the UV-vis spectra in 200-300 nm. (e) Temperature changes of PBS and AuNCs/SV solution with 808 nm laser irradiation (1.5 W/cm^2). (f) The encapsulation efficiency of SV ($n = 3$).

work established a possibility that AuNCs-based PTT can be used to amplify PTT-immunotherapy.

The AuNCs/SV were synthesized with the following steps. Briefly, 28.5 nm AgNPs were developed firstly [31]. Then we synthesized AuNCs on the basis of AgNPs with the help of $HAuCl_4$ [32,33]. As shown in Fig. 2a, transmission electron microscope (TEM) image of the AuNCs clearly showed a hollow mesoporous structure. Furthermore, the Au, Ag, N and C elements were distributed in AuNCs (Fig. 2b), suggesting the successful etching on AgNPs for the construction of AuNCs. Then, the size of AuNCs/SV was confirmed to be about 50 nm by dynamic light scattering analysis (DLS, Fig. 2c). The UV absorption spectrum (Fig. 2d) of AuNCs showed a new broad peak between 200 nm and 300 nm, indicating that SV was loaded into AuNCs. Subsequently, the photothermal conversion of AuNCs/SV was detected. When AuNCs solution (50 μg/mL) was irritated with NIR laser (808 nm) for 5 min, its temperature increased from 25.0 °C to 55.4 °C, while the temperature of deionized water has no obvious change (Fig. 2e). As shown in Fig. 2f, when the feed of AuNCs and SV ratio was increased to 1/1, the entrapment efficiency did not increase significantly and the entrapment efficiency of SV reached to ~22%.

Antigen capture and LN-targeting ability of AuNCs/SV are crucial for stimulating effective cancer treatment. We first evaluated the formation of *in situ* recombinant NPs. The TEM image (Fig. 3a) of AuNCs/SV with laser irradiation showed that there was a halo covered the original AuNCs. And the zeta potential and size (Figs. 3b and c) of AuNCs/SV changed obviously after laser irradiation, hinting that the AuNCs/SV captured TAAs successfully. Gel electrophoresis (Fig. 3d) showed that the proteins captured by AuNCs were different from those of B16-F10 cell lysates. To further confirm the presence of specific antigens on the AuNCs-bound proteins, the mass spectrometry was performed to determine if any of the captured proteins contained antigens expressed by B16-F10 cells. As shown in Fig. 3e, there were many neoantigens and DAMPs being detected which were in favor of the immune effect [34,35]. Then western blotting analysis (Fig. 3f) was adopted on tumor-specific antigens (Tnpo3 and Cpsf3l) that could initiate antitumor immune response. These results proved

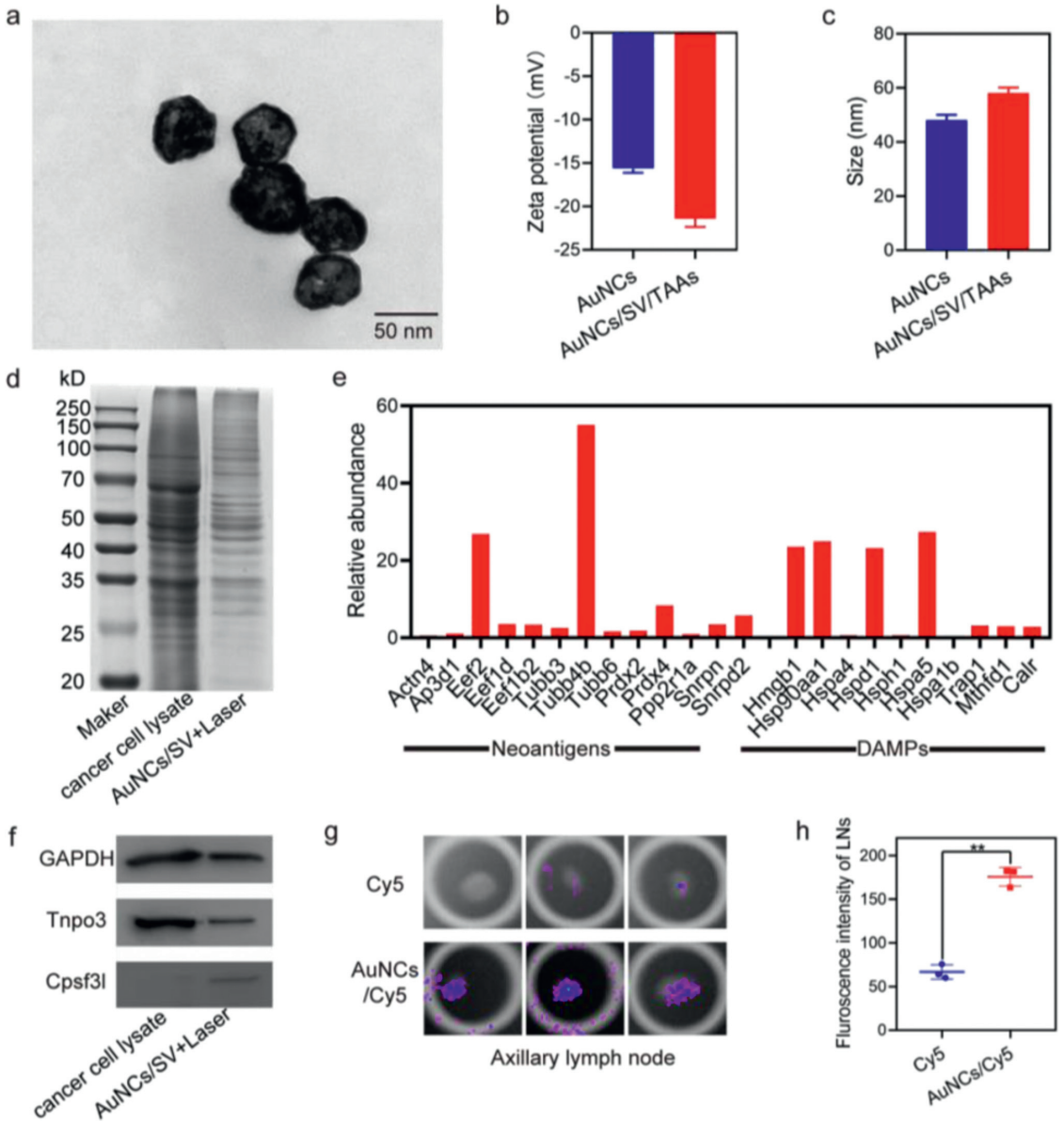

Fig. 3. (a) TEM image, (b) zeta potential and (c) size of AuNCs/SV/TAAs. (d) Gel electrophoresis analysis of B16-F10 cancer cell lysate and AuNCs/SV under 808 nm laser. (e) Protein relative abundance analysis of AuNCs/SV/TAAs. (f) Western blotting analysis of B16-F10 tumor-specific antigens (Tnpo3 and Cpsf3l) in AuNCs/SV/TAAs. (g) Image and (h) quantification of the fluorescence intensity of axillary LNs after intratumoural injection for 12 h ($n = 3$).

that the *in situ* effective recombinant NPs could be successfully constructed.

Afterwards, to confirm that AuNCs could deliver TAAs to LNs, we injected Cy5 labeled-AuNCs intratumourally to study the efficiency of lymphatic drainage. The fluorescence intensity of AuNCs/SV/Cy5 group was obviously stronger than free Cy5 at 12 h post-administration (Figs. 3g and h), showing AuNCs could easily deliver antigens to nearby LNs (axillary LNs), which was instrumental in augmenting systemic immune response.

In addition, we investigated the cellular uptake of isothiocyanate (FITC)-labeled AuNCs in B16-F10 cells by flow cytometry and microscope. As depicted in Fig. 4a, the fluorescence intensity in cells increased in a time-dependent manner. And at 4 h, we found that the presence of AuNCs/SV could enhance the uptake of preparations compared with the FITC group (Fig. 4b). In order to study the effect of 808 nm laser on cell proliferation, MTT (3-(4,5-dimethylthiazol-2-yl)-2,5-diphenyltetrazolium bromide) assay was chosen to evaluate cell viability. AuNCs/SV group showed less cytotoxic to tumor cells (with cell viability higher than 92%) (Fig. 4c). However, after laser irradiation, AuNCs/SV exhibited the significant cytotoxicity, and only approximately 12.1% of the cells were alive at the AuNCs concentration of 60 μg/mL, indicating that the combination of AuNCs/SV and NIR could effectively kill tumor cells. Then the expression level of immunogenic cell death (ICD) makers, including calreticulin (CRT) and high mobility group box 1 (HMGB1), were determined by flow cytometry and enzyme-linked immunosorbent assay respectively [36,37]. Flow cytometry examination showed that AuNCs/SV with laser treatment induced ~3.5-fold higher CRT expression than the control group (Fig. 4d). The extracellular HMGB1 of AuNCs/SV with laser treatment group was ~1.7-fold higher than control group (Fig. 4e). All these results consistently verified that AuNCs-based PTT could effectively induce ICD *in vitro*. It has reported that DCs support antitumor adaptive immunity by presenting antigen and stimulating T cells [38,39], and then ICD-induced DCs maturation was examined by flow cytometry. The mature DCs frequency of AuNCs/SV+Laser group was

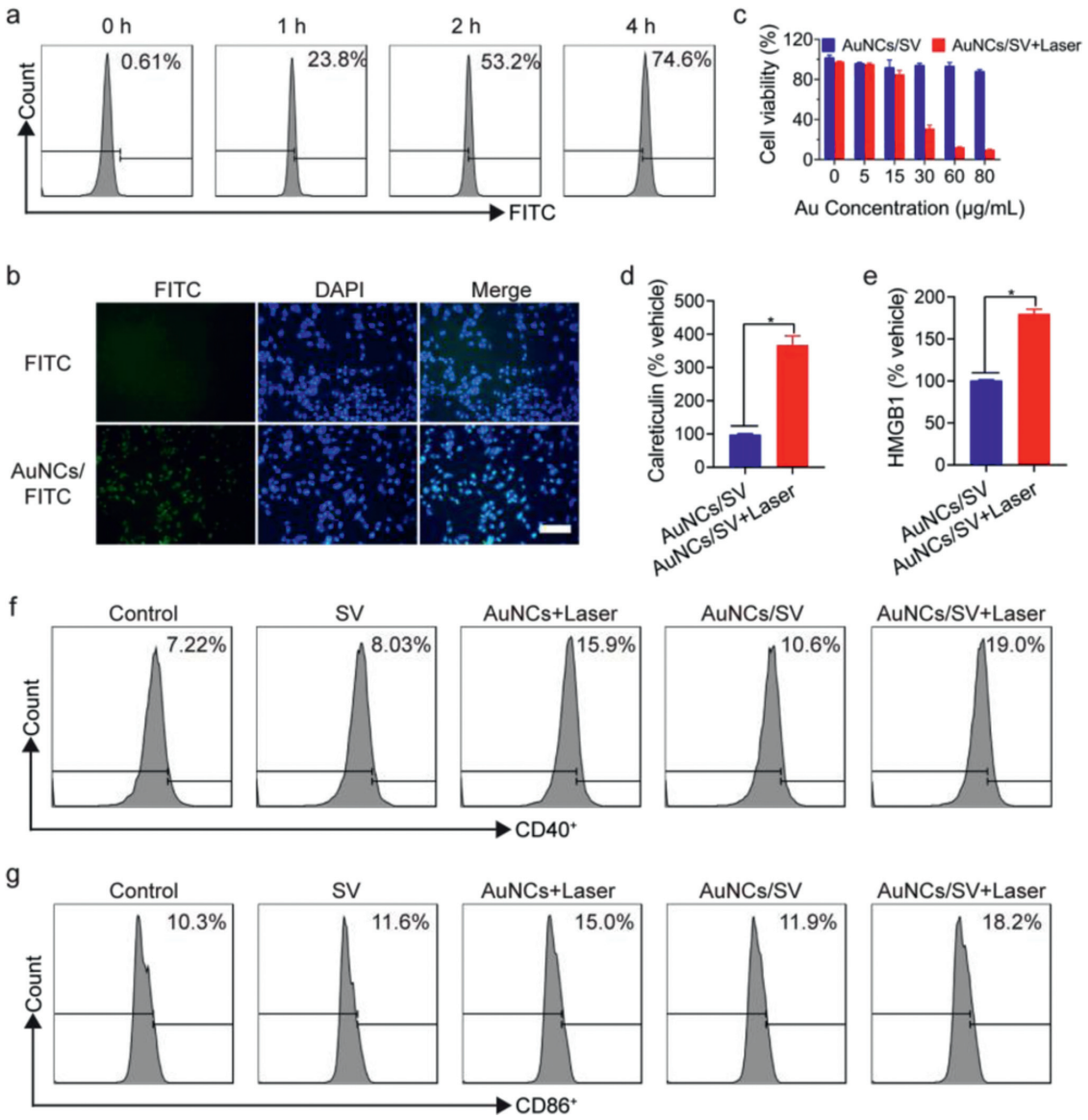

Fig. 4. (a) Cellular uptake of FITC detected by flow cytometry. (b) Fluorescence images of B16-F10 cells treated with FITC, AuNCs/FITC for 4 h. (c) Cell viability of B16-F10 cells treated with AuNCs/SV, AuNCs/SV+Laser under different concentrations. (808 nm laser, 2 min, 1.5 W/cm^2, $n = 6$). The investigation of CRT expression (d) and HMGB1 secretion (e). Data represent mean ± SD ($n = 3$). Quantification of CD40 (f) and CD86 (g) expression on the surface of DCs after different treatment by flow cytometry. Data represent mean ± SD ($n = 3$). $^*P < 0.05$.

higher than other groups (Figs. 4f and g), indicating that tumor-ICD induced by AuNCs/SV with PTT could efficiently promote DCs maturation. Above results suggested that AuNCs/SV were likely to become a promising PTT agent and further trigger downstream immune responses.

Inspired by the highly therapeutic efficiency and the antitumor immune responses *in vitro*, we next evaluated the synergistic antitumor efficiency of AuNCs/SV with NIR on B16F10-bearing C57 mice. All animal experiments were strictly conducted according to the guidelines stipulated and approved by Henan laboratory animal center. Moreover, when saline, SV, AuNCs, AuNCs+SV or AuNCs/SV were intratumorally injected, the groups containing AuNCs were irradiated with a NIR laser (1.5 W/cm^2). Then the tumor volume and body weight were recorded every other day, and the survival time of all experimental groups was still inspected after 5 times of administrations. As shown in Fig. 5a, according to the tumor volume change profiles, both the tumor volumes in saline-treated and SV-treated groups showed a rapidly increase over 14 days, while the AuNCs with laser irradiation exhibited certain tumor growth delay due to PTT-mediated tumor cells damage. However, the AuNCs/SV treated mice with laser irradiation displayed obvious tumor inhibition compare to AuNCs+SV+Laser group and AuNCs+Laser group, which was due to the direct tumor killing effect induced by PTT and the existence of adjuvant SV [40]. After AuNCs/SV with laser treatment, the tumor cells could be lysed into large amount of tumor debris to release TAAs. The *in situ* tumor vaccine formed by AuNCs/SV and released TAAs could induce strong anti-tumor immune response, and further remove the residual tumor cells, showing prolonged survival time in AuNCs+SV+Laser group (Fig. 5b). The hematoxylin and eosin (H&E) staining of tumors (Fig. S1 in Supporting information) were performed to confirm the therapeutic effects. Furthermore, the weight of all treated mice showed no significant change during the period of treatment (Fig. S2 in Supporting information) and the H&E staining of major organs showed

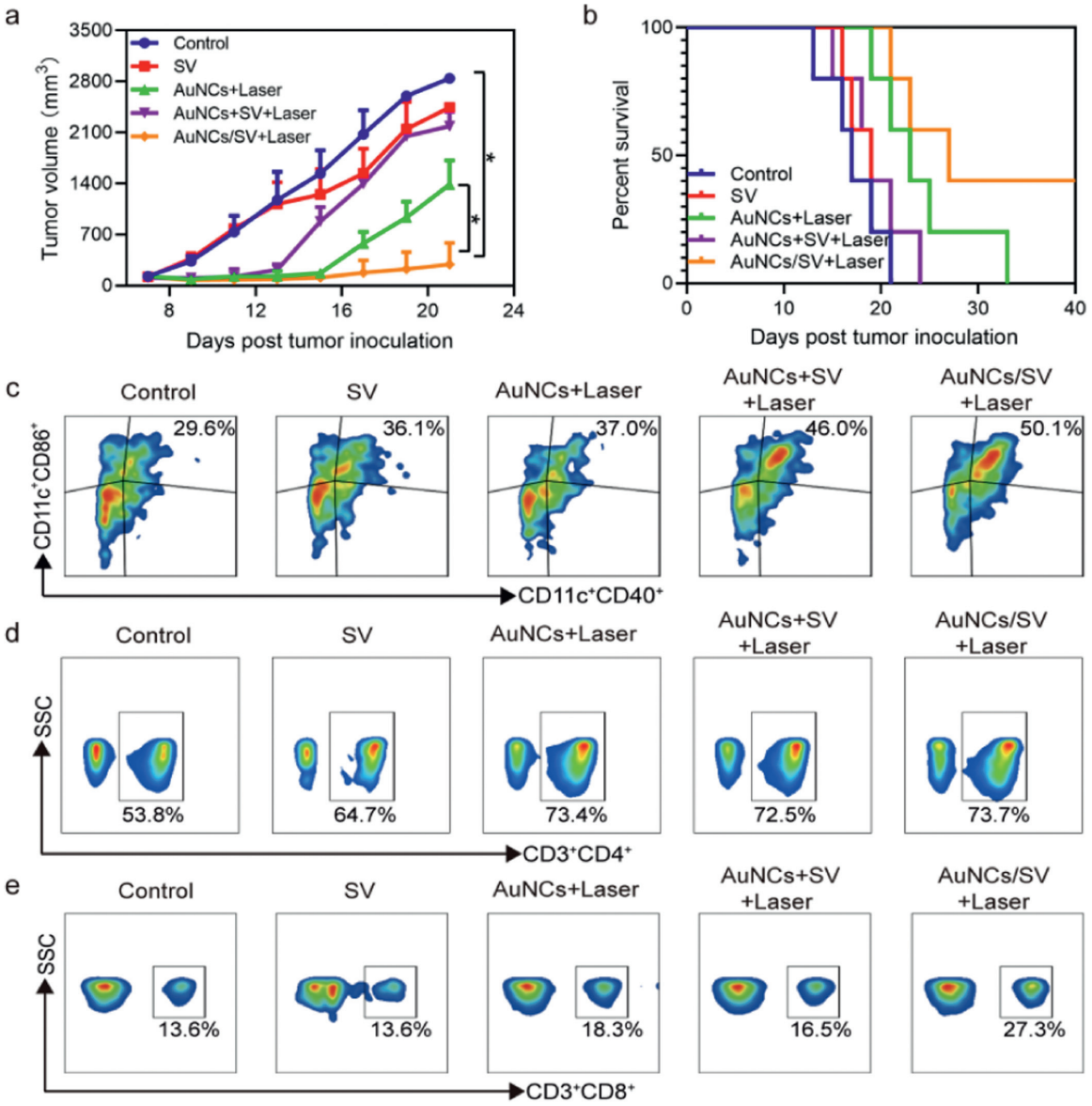

Fig. 5. (a) Tumor size and (b) survival curves of B16-F10 tumor-bearing mice in different groups ($n = 5$). The populations of (c) DCs maturation ($CD11c^+CD40^+CD86^+$), (d) $CD4^+$ T cells ($CD3^+CD4^+$) and (e) $CD8^+$ T cells ($CD3^+CD8^+$) in LNs of mice after various treatments. Data represent mean ± SD ($n = 3$). $^*P < 0.05$.

no noticeable organ damage in the group containing AuNCs (Fig. S3 in Supporting information), indicating the excellent biocompatibility and minimal toxicity.

Next, we carefully studied the anti-tumor immune response induced by AuNCs/SV downstream, including mature DCs and activated T cells in tumor and LNs after 3 times of administration. As shown in Fig. S4a (Supporting information), an obviously increase of mature DCs in tumors could be observed in the AuNCs/SV with NIR laser irradiation compared with other groups. This was due to the co-delivery of antigen and adjuvant. $CD8^+$ T cells and $CD4^+$ T cells are the main effector cells of anti-tumor immune response, which can be activated by mature DCs [41,42]. Therefore, we further evaluated the number of infiltrating T cells at tumor site. As expected, compared with any other treatment group, more mature DCs, $CD8^+$ T cells and $CD4^+$ T cells were found in the tumor site after the treatment of AuNCs/SV with NIR laser (Figs. S4b, S4c and S5 in Supporting information), which was owing to the synergistic effect of TAAs and SV.

Especially in PTT induced vasodilation, AuNCs/SV/TAAs of ~55 nm could be advantageous to drained to the LNs and enhance the body's immunity, so some immune cells in LNs were investigated. As shown in Fig. 5c, AuNCs/SV with laser group significantly enhanced the expression of CD40 and CD86 in LNs, which were almost twice higher than control group. These data demonstrated that the construction of *in situ* recombinant NPs improved DCs activation. After primed by antigens, mature DCs would trigger the following immune response and process antigens into MHC–peptide complex to present to T cells [43,44]. Therefore, as shown in Figs. 5d and e, AuNCs/SV under laser irradiation significantly enhanced $CD4^+$ and $CD8^+$ T-cell proliferation compared to control, SV, AuNCs with laser and the AuNCs+SV with laser groups (Fig S6 in Supporting information), indicating that AuNCs/SV/TAAs NPs promoted the differentiation and proliferation of T lymphocytes in LNs effectively. The results also showed the recombinant NPs were easy to migrate to LNs and activate T cells obviously. Moreover, immunofluorescence assay (Fig. S7 in Supporting information) was conducted to confirm the increase of the percentage of $CD8^+$ T cells, indicating that the co-delivery of TAAs and SV improved the activation of $CD8^+$ T cells in LNs. Altogether, these results demonstrated that the *in situ* NP recombinant strategy based on AuNCs/SV

with 808 nm laser irradiation enhanced PTT effect by improving the immune responses.

In summary, *in situ* NP recombinant strategy based on AuNCs was developed for enhancing PTT effect. AuNCs/SV with NIR treatment could kill tumor cells directly and promote TAAs release. And the released TAAs could be then captured by AuNCs/SV to construct AuNCs/SV/TAAs which were ingested by DCs, significantly inducing strong antitumor immunity. Besides, AuNCs/SV/TAAs exhibited good LN-targeting ability, which promoted the maturation of DCs and enhanced the cytotoxic T lymphocytes obviously. Moreover, study on pharmacodynamics showed that AuNCs/SV+Laser group could effectively inhibit tumor growth and prolong the survival time of mice. Therefore, we believe that the therapeutic strategy might provide a new way for enhancing PTT-immunotherapy and facilitating the development of autologous anticancer vaccines.

Declaration of competing interest

The authors declare that they have no known competing financial interests or personal relationships that could have appeared to influence the work reported in this paper.

Acknowledgments

This project was financially supported by the National Natural Science Foundation of China (Nos. U1804183, 81901878 and 81874304), China Postdoctoral Science Foundation (No. 2019M662553) and Key Scientific Research Project (Education Department of Henan Province, No. 20HASTIT049).

Supplementary materials

Supplementary material associated with this article can be found, in the online version, at doi:10.1016/j.cclet.2021.07.025.

References

[1] C. Kim, E.C. Cho, J. Chen, et al., ACS Nano 4 (2010) 4559–4564.
[2] J. Ferlay, I. Soerjomataram, R. Dikshit, et al., Int. J. Cancer 136 (2015) E359–E386.
[3] F. Bray, J. Ferlay, I. Soerjomataram, et al., CA-Cancer J. Clin. 68 (2018) 394–424.
[4] S. Luo, Y. Zhu, Y. Li, et al., J. Biomed. Nanotechnol. 16 (2020) 842–852.
[5] W. Ou, L. Jiang, R.K. Thapa, et al., Theranostics 8 (2018) 4574–4590.
[6] L. Luo, C. Zhu, H. Yin, et al., ACS Nano 12 (2018) 7647–7662.
[7] D. Hu, L. Chen, Y. Qu, et al., Theranostics 8 (2018) 1558–1574.
[8] L. Shen, T. Zhou, Y. Fan, et al., Chin. Chem. Lett. 31 (2020) 1709–1716.
[9] T. Guo, W. Lin, W. Chen, et al., J. Biomed. Nanotechnol. 16 (2020) 1219–1228.
[10] Q. Chen, L. Xu, C. Liang, et al., Nat. Commun. 7 (2016) 13193.
[11] R. Ge, C. Liu, X. Zhang, et al., ACS Appl. Mater. Inter. 10 (2018) 20342–20355.
[12] J. Peng, Y. Xiao, W. Li, et al., Adv. Sci. (Weinh) 5 (2018) 1700891.
[13] X. Jiang, Z. Dai, Chin. Sci. Bull. 63 (2018) 1783–1802.
[14] Y. Cheng, Q. Chen, Z. Guo, et al., ACS Nano 14 (2020) 15161–15181.
[15] X. Zheng, D. Pan, M. Chen, et al., Adv. Mater. 31 (2019) e1901586.
[16] J. Wu, D.H. Bremner, S. Niu, et al., J. Biomed. Nanotechnol. 15 (2019) 1415–1431.
[17] M. Zhou, Y. Zhou, Y. Cheng, et al., J. Biomed. Nanotechnol. 16 (2020) 739–762.
[18] H. Zhao, B. Zhao, L. Wu, et al., ACS Nano 13 (2019) 12553–12566.
[19] L. Chen, X. Ma, M. Dang, et al., Adv. Healthc. Mater. 8 (2019) e1900039.
[20] Y. Du, Y. Xia, Y. Zou, et al., ACS Nano 13 (2019) 13809–13817.
[21] A.V. Kroll, R.H. Fang, Y. Jiang, et al., Adv. Mater. 29 (2017) e1703969.
[22] M. Luo, L.Z. Samandi, Z. Wang, et al., J. Control. Release 263 (2017) 200–210.
[23] R. Liang, J. Xie, J. Li, et al., Biomaterials 149 (2017) 41–50.
[24] L. Zeng, Z. Liao, W. Li, et al., Chin. Chem. Lett. 31 (2020) 1162–1164.
[25] Y. Wu, F. Li, X. Zhang, et al., Carbohyd. Polym. 255 (2021) 117490.
[26] X. Qian, A. Levenstein, J.E. Gagner, et al., Langmuir 30 (2014) 1295–1303.
[27] W. Li, H. Zhang, X. Guo, et al., ACS Appl. Mater. Inter. 9 (2017) 3354–3367.
[28] Y. Yu, Z. Zhang, Y. Wang, et al., Acta Biomater. 59 (2017) 170–180.
[29] Q. Chen, H. Qi, Y.T. Ren, et al., AIP Adv. 7 (2017) 065115.
[30] X. Ke, G.P. Howard, H. Tang, et al., Adv. Drug Deliv. Rev. 151-152 (2019) 72–93.
[31] Y. Xia, Y. Xie, Z. Yu, et al., Cell 175 (2018) 1059–1073.
[32] Y. Wan, Z. Guo, X. Jiang, et al., J. Colloid Interface Sci. 394 (2013) 263–268.
[33] Y. Xia, W. Li, C.M. Cobley, et al., Acc. Chem. Res. 44 (2011) 914–924.
[34] L. Dong, Y. Li, Z. Li, et al., ACS Appl. Mater. Inter. 10 (2018) 9247–9256.
[35] Y. Min, K.C. Roche, S. Tian, et al., Nat. Nanotechnol. 12 (2017) 877–882.
[36] J. Yu, Y. Kong, J. Guo, Chin. J. Immunol. 35 (2019) 2156–2162.
[37] X. Ju, X. Liu, J. Nanjing Med. Univ. Nat. Sci. Ed. 40 (2020) 1070–1073.
[38] S. Chattopadhyay, Y.H. Liu, Z.S. Fang, et al., Nano Lett. 20 (2020) 2246–2256.
[39] O.P. Joffre, E. Segura, A. Savina, et al., Nat. Rev. Immunol. 12 (2012) 557–569.
[40] R.B. Patel, M. Ye, P.M. Carlson, et al., Adv. Mater. 31 (2019) e1902626.
[41] X. Dong, J. Liang, A. Yang, et al., ACS Appl. Mater. Inter. 11 (2019) 4876–4888.
[42] Y.X. Zhang, Y.Y. Zhao, J. Shen, et al., Nano Lett. 19 (2019) 2774–2783.
[43] S.Y. Kim, H. Phuengkham, Y.-W. Noh, et al., Adv. Funct. Mater. 26 (2016) 8072–8082.
[44] D. Dersh, J. Holly, J.W. Yewdell, Nat. Rev. Immunol. 21 (2020) 116–128.